Quantum theory of optical-pulse propagation through an amplifying slab

Maurizio Artoni[1,2] and Rodney Loudon[1]
[1]*Department of Physics, University of Essex, Colchester CO4 3SQ, United Kingdom*
[2]*CSIC, Instituto de Estructura de la Materia, Serrano 123, 28006 Madrid, Spain*
(Received 29 August 1997)

We calculate the effects of normal transmission through an amplifying dielectric slab on the properties of an incident pulse of light. The transmitted pulse shows shifts in peak position and additional lengthening or shortening with respect to the unamplified incident pulse. The magnitudes of these effects are generally larger than those of the corresponding changes that occur in transparent or attenuating slabs. They are interpreted in terms of the interference of multiply reflected contributions to the transmitted pulse. The theory is valid for pulses of nonclassical light, but the same reshaping occurs for appropriate pulses of classical light.
[S1050-2947(98)05501-2]

PACS number(s): 42.50.−p

I. INTRODUCTION

The tunneling of a particle through a barrier is a problem of continued interest, and one that exhibits striking features. In particular, photon tunneling through a multilayer dielectric structure has recently attracted much interest: a photon wave packet that has ''tunneled'' through a one-dimensional photonic band-gap barrier can be peaked at a shorter time delay than its ''twin-photon'' wave packet that has propagated through the same distance in air [1]. The effect is a consequence of pulse reshaping and, although the apparent tunneling velocity is superluminal, this is not a genuine signal velocity and Einstein causality is not violated. Attenuation or amplification play important roles in the peak shift and in the broadening or narrowing of the transmitted pulse. The theory of pulse propagation through a bounded attenuating medium, originally due to Halevi and co-workers [2–4], has recently been extended by others in more detailed treatments of the effects of attenuation and multiple reflections at the sample surfaces, including their roles in the apparent superluminal pulse propagation through multilayer dielectric barriers [5–8].

Pulse propagation through an amplifying medium, however, has received less attention. Superluminal propagation in a transparent spectral region outside the resonance of an inverted two-level atomic medium has been discussed previously [9–14]. Superluminal pulse propagation in an active plasma acting as a nonlinear amplifier has also been examined [15], and there is long-standing experimental work on subluminal pulse propagation inside the gain band of a xenon discharge [16]. We have recently developed a quantum theory of the electromagnetic field in bounded dielectrics that exhibit amplification over some range of frequencies. Despite the practical differences between attenuation and amplification, a uniform theoretical formalism applies across the complete range of positive frequencies [17–19]. We use the formalism here to examine the effects of propagation through an amplifying dielectric slab on an incident light pulse. Multiple reflections at the slab surfaces again cause an apparent delay or advance and broadening or narrowing of the pulse, similar to the effects found for a transparent or attenuating slab but enhanced by amplification.

The main expressions needed from the field quantization are briefly stated in Sec. II, and the theory of pulse transmission through an amplifying slab is presented in Sec. III. The physical interpretation of the results is discussed in Sec. IV, where we provide analytical expressions that allow for a straightforward understanding of how the pulse parameters are affected by amplification as compared to attenuation. Our main interest is in the reshaping of the pulse caused by multiple reflections inside the slab. In order to display these ''surface'' effects most clearly, we ignore the dispersion in the dielectric function, which can produce an additional ''bulk'' reshaping of the incident pulse. The main conclusions of the work are summarized in Sec. V.

II. FIELD QUANTIZATION

The electromagnetic field in an amplifying slab is quantized on the basis of a continuous set of plane waves propagating in the direction perpendicular to the surfaces of the slab defined by the dielectric function

$$\varepsilon(x,\omega)=\begin{cases} n^2(\omega)=[\eta(\omega)+i\kappa(\omega)]^2 & \text{for } |x|<l \\ 1 \qquad \text{for } |x|>l. \end{cases} \tag{1}$$

The extinction coefficient $\kappa(\omega)$ is generally positive for most frequencies ω, corresponding to attenuation, but it may be negative over limited ranges of frequency, corresponding to amplification by the dielectric material. For the latter frequencies reflection or transmission at the slab may produce amplification of an incident light beam.

For propagation in the direction of the positive x axis, the positive frequency part of the vector potential operator in the transmission region $x>l$ is given for all frequencies ω by [17,19]

$$\hat{A}^{(+)}(x,t)=\int_0^\infty d\omega\left(\frac{\hbar}{4\pi\varepsilon_0 c\omega S}\right)^{1/2} \times[\hat{b}_R(\omega)e^{i\omega x/c}+\hat{b}_L(\omega)e^{-i\omega x/c}]e^{-i\omega t}, \tag{2}$$

where S is an area of quantization in the yz plane. The notation for the destruction operators used in the quantization is

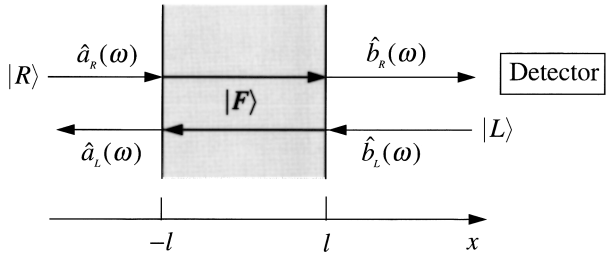

FIG. 1. Spatial configuration of the dielectric slab, and notation for the destruction operators and input states used in the quantization of the electromagnetic field.

shown in Fig. 1. The operators $\hat{a}_R(\omega)$, $\hat{b}_L(\omega)$ and $\hat{a}_L(\omega)$, $\hat{b}_R(\omega)$ represent the pairs of input and output fields, respectively, and we denote the states of the input fields by $|R\rangle$ and $|L\rangle$. The rightward- and leftward-propagating outgoing field operators,

$$\hat{b}_R(\omega)=R(\omega)\hat{b}_L(\omega)+T(\omega)\hat{a}_R(\omega)+\hat{F}_R(\omega) \tag{3}$$

and

$$\hat{a}_L(\omega)=T(\omega)\hat{b}_L(\omega)+R(\omega)\hat{a}_R(\omega)+\hat{F}_L(\omega), \tag{4}$$

respectively, are related to the input fields through the complex amplitude reflection and transmission coefficients $R(\omega)$ and $T(\omega)$.

The intensity gain coefficients for the light transmitted through or reflected from the slab are defined by

$$G_T(\omega)=|T(\omega)|^2 \quad \text{and} \quad G_R(\omega)=|R(\omega)|^2, \tag{5}$$

where for convenience we use the term ''gain'' even when the coefficients are smaller than unity. We consider particularly transmission through the slab, where the gain is determined by

$$T(\omega)=\frac{4n(\omega)}{D(\omega)}\exp\left\{\frac{2i\omega[n(\omega)-1]l}{c}\right\}, \tag{6}$$

with

$$D(\omega)=[n(\omega)+1]^2-[n(\omega)-1]^2\exp[4i\omega n(\omega)l/c]. \tag{7}$$

Figure 2 shows the form of the transmission gain as a function of the refractive index $\eta(\omega)$ for a fixed frequency and three values of $\kappa(\omega)$.

The operators $\hat{F}_R(\omega)$ and $\hat{F}_L(\omega)$ in Eqs. (3) and (4), proportional to $\sqrt{|\kappa(\omega)|}$ [19], represent the outgoing rightward- and leftward-propagating noise fields produced inside the slab. The state of the noise field, denoted by $|F\rangle$, has strictly the nature of a statistical mixture. The minimum noise at attenuated frequencies vanishes for zero temperature. For amplified frequencies, the noise is minimized for zero effective temperature, corresponding to complete population inversion, with a rightward noise operator correlation

$$\langle\hat{F}_R^\dagger(\omega)\hat{F}_R(\omega')\rangle=\{G_T(\omega)+G_R(\omega)-1\}\delta(\omega-\omega'). \tag{8}$$

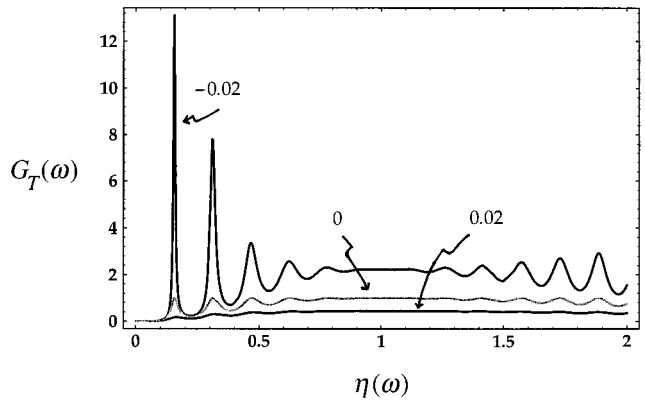

FIG. 2. Transmission gain $G_T(\omega)$ as a function of the real refractive index $\eta(\omega)$ for the values of extinction coefficient $\kappa(\omega)$ shown. The frequency ω and the slab thickness $2l$ are such that $\omega l/c=10$.

This additive noise contribution for amplified frequencies is neglected in the following calculations (see Refs. [6,14,19] for further discussions of the noise).

III. PULSE TRANSMISSION

Consider an input where the states of the field impinging leftward and rightward on the slab are, respectively, a conventional vacuum $|L\rangle=|0\rangle$ and a photon-number state wave packet of length L with a Gaussian frequency distribution centered on the carrier frequency ω_c,

$$|R\rangle=\frac{L^{N/2}}{(2\pi c^2)^{N/4}\sqrt{N!}}\times\left[\int_0^\infty d\omega\ \exp[-L^2(\omega-\omega_c)^2/4c^2]\hat{a}_R^\dagger(\omega)\right]^N|0\rangle. \tag{9}$$

Single-photon states of this form can be realized experimentally [20]. They have been employed in the successful demonstration of superluminal tunneling through a one-dimensional photonic band-gap material [1].

The effects of propagation are most directly studied by evaluating the normal-order Poynting vector, whose expectation value for the wave packet (9), after transmission through the slab, is

$$\langle:\hat{S}(x,t):\rangle=\frac{\hbar NL}{(2\pi)^{3/2}cS}\left|\int_0^\infty d\omega\ \omega^{1/2}T(\omega)\times\exp\left\{-i\omega\left(t-\frac{x}{c}\right)-\frac{L^2(\omega-\omega_c)^2}{4c^2}\right\}\right|^2. \tag{10}$$

The integral can be carried out following a procedure similar to that developed in Ref. [6]. The incident pulse is assumed to be much longer than the optical thickness of the slab ($L\gg 2l\eta/\pi$), and with a frequency spread much smaller than the carrier frequency ($c/L\ll\omega_c$). When the transmission amplitude $T(\omega)$ has a negligible variation over the main fre-

quencies that make up the pulse, the optical wave vector can be expanded around the pulse carrier frequency ω_c in the usual way:

$$k(\omega)\equiv\frac{\omega n(\omega)}{c}\cong k_c+(k'_{cr}+ik'_{ci})(\omega-\omega_c), \qquad (11)$$

where $k_c=\omega_c n_c/c$ and $n_c\equiv n(\omega_c)$. The prime denotes the frequency derivative of the wave vector, and this is divided into its real and imaginary parts; the real part is the inverse of the group velocity at the carrier frequency. Dispersion in the refractive index $\eta(\omega)$ around its value $\eta_c\equiv\eta(\omega_c)$ and in the extinction coefficient $\kappa(\omega)$ around $\kappa_c\equiv\kappa(\omega_c)$ are neglected in the following, and we set $k'_{cr}\to\eta_c/c$ (inverse phase velocity) and $k'_{ci}\to\kappa_c/c$.

The resulting expression for the Poynting vector retains a single component with Gaussian shape after transmission through the slab, with the form

$$\langle:\hat{S}(x,t):\rangle=S_0\mathscr{T}\exp\{-2(ct-x+\Delta x)^2/(L^2+\Delta L^2)\}. \qquad (12)$$

Here $S_0=Nc\hbar\omega_c/LS\sqrt{\pi/2}$ is the peak power density of the incident pulse, while $\mathscr{T}$ determines how the peak intensity scales through the slab. There appear in Eq. (12) a shift Δx in the position of the peak of the pulse from its vacuum value ct and a change ΔL^2 in the mean-square spatial length of the transmitted pulse from its incident value L^2. These have complicated analytic expressions, similar to results given in Ref. [6] for an attenuating slab, which are not explicitly given here but are plotted instead in Fig. 3.

In Fig. 3(a) we compare how the peak shift Δx after propagation through the slab varies as a function of η_c for a positive (attenuation), vanishing (transparent), and two negative (amplification) values of κ_c. The shift oscillates as a function of η_c around the mean value $2l(1-\eta_c)$ associated with the change in optical path caused by the refractive index of the slab, and the amplitude of the oscillations increases with $|\eta_c-1|$. The amplitude becomes appreciably larger for increasing values of the amplification and, for the parameters used here, its largest value is of the order of three times the slab thickness. Likewise Fig. 3(b) illustrates the variations in the mean-square length $L_T^2=L^2+\Delta L^2$ of the transmitted pulse. Transmission through the slab may shorten or lengthen the pulse depending on the value of the real refractive index η_c, particularly for larger values of $|\eta_c-1|$; again, increasing values of the amplification enhance the change in length from that of the incident pulse. For the higher amplification shown, with $\kappa_c=-0.04$, the largest change in mean-square length is more than an order of magnitude greater than that for $\kappa_c=0$. The amplitudes of the oscillations in both peak shift and mean-square length are thus significantly increased by the amplification relative to their values for a transparent dielectric. By contrast, attenuation with $\kappa_c=0.02$ reduces the amplitudes of the oscillations relative to their values for a transparent dielectric [6].

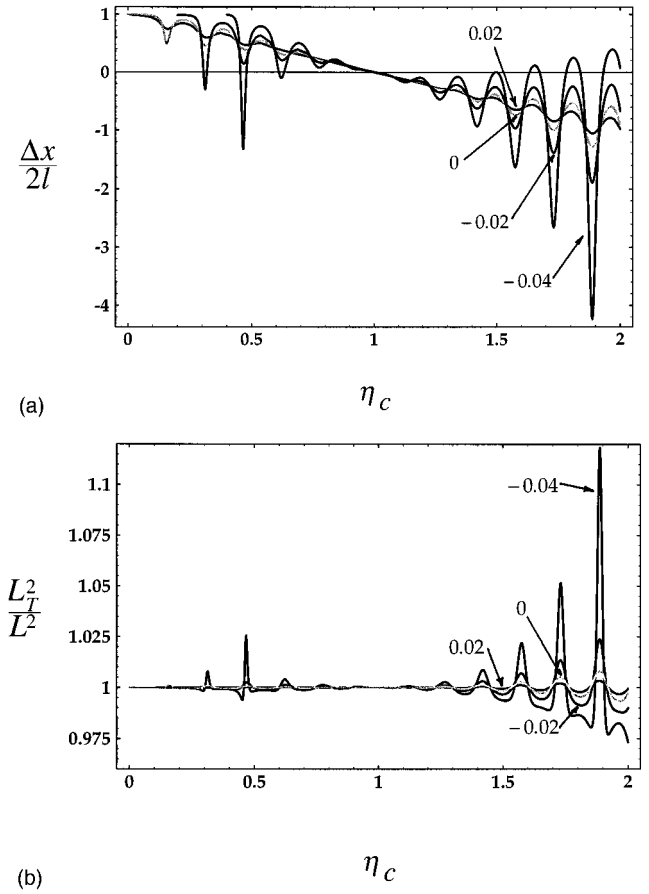

FIG. 3. Properties of a Gaussian pulse of input length $L=40l$ and carrier frequency $\omega_c=10c/l$ after transmission through the slab as functions of the real refractive index η_c for the extinction coefficients κ_c shown against the curves, (a) relative shift in the peak position and (b) mean-square length.

IV. INTERPRETATION

In this section we analyze the oscillations found in Fig. 3 and, in particular, we derive approximate analytical expressions for the minima and maxima of the peak shift and mean-square length of the transmitted pulse, the main parameters of experimental interest. Maxima (minima) of the mean-square length correspond to minima (maxima) of the peak shift; maxima of L_T^2 occur in turn at points of maximum transmission gain (cf. Fig. 2) where the magnitude of $D_c\equiv D(\omega_c)$ in Eq. (7) is a minimum. It is instructive to express

$$|D_c|^2=|n_c+1|^4\{1+|g_c|^2-2|g_c|\cos\phi_c\} \qquad (13)$$

in terms of

$$g_c=g(\omega_c)=\left(\frac{n_c-1}{n_c+1}\right)^2\exp[4in_c\omega_c l/c]\equiv|g_c|e^{i\phi_c}, \qquad (14)$$

the complex round-trip gain or loss for light that travels from a point in the slab and back to the same point after two surface reflections. For a fixed extinction coefficient κ_c and ratio $\omega_c l/c$, $|D_c|^2$ is an oscillating function of the real refractive index η_c with period $\pi c/2\omega_c l$ and extrema for

$$\cos\,\phi_c=\pm 1,\quad \frac{4\,\eta_c\omega_c l}{c}=\pi m-2\,\tan^{-1}\left(\frac{2\,\kappa_c}{\eta_c^2+\kappa_c^2-1}\right),$$

$$m=\begin{cases}\text{even integer}\\ \text{odd integer.}\end{cases} \qquad (15)$$

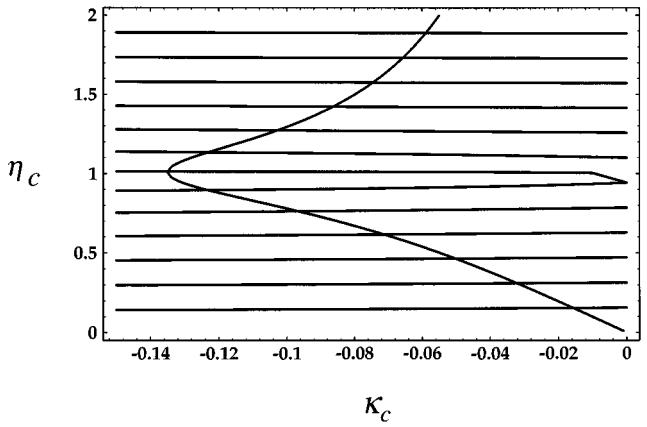

FIG. 4. The family of approximately horizontal lines and the curved line represent, respectively, the values of the real refractive index and extinction coefficient that satisfy conditions (16) and (17) for $\omega_c l/c=10$. The intersection points give the values of η_c and κ_c for which an amplifying slab of thickness $2l$ has lasing thresholds at frequency ω_c.

The upper and lower alternatives in Eq. (15) correspond to minima and maxima, respectively, in the shift Δx, and vice versa for the mean-square length L_T^2.

Both Δx and L_T^2 are singular when the right-hand side of (13) vanishes, that is, when

$$\cos\,\phi_c=1 \tag{16}$$

and

$$|g_c|=1, \quad \frac{(\eta_c-1)^2+\kappa_c^2}{(\eta_c+1)^2+\kappa_c^2}=\exp\left(\frac{4\kappa_c\omega_c l}{c}\right) \tag{17}$$

are simultaneously satisfied. Condition (16) specifies phase matching of the light after a round trip in the slab, and it is satisfied for values of the refractive index and extinction coefficient that lie on the set of approximately horizontal lines in Fig. 4. Condition (17) specifies a gain in the dielectric that is sufficient to offset the loss of optical energy through the slab surfaces, and it is satisfied for values of η_c and κ_c that lie on the curved line of Fig. 4. As discussed in Ref. [19], the state of the optical field in the amplifying slab transforms into one of self-sustaining oscillation when the two conditions are simultaneously satisfied: thus Eqs. (16) and (17) determine the thresholds for laser action at the frequencies ω_c identified by the intersection points in Fig. 4. The high transmission gain shown in Fig. 2 for $\kappa(\omega)=-0.02$ and $\eta(\omega)=0.16$ is a consequence of the proximity of these parameters to values for which the amplifying slab has a lasing threshold. The theory given here is valid only for material parameters for which the conditions for laser action are not satisfied for any frequency, so that $|g_c|<1$. The curves in Figs. 3(a) and 3(b) for $\kappa_c=-0.02$ and -0.04 are truncated at $\eta_c=0.2$ and 0.4, respectively, to avoid the lasing singularities.

For realistic values of the material parameters, $|\kappa_c|$ is generally much less than unity for both amplified and attenuated frequencies, and we derive approximate expressions for Δx and L_T^2 in this limit. The trigonometric term in Eq. (15) can now be ignored, and for $4\eta_c\omega_c l/c\cong\pi m$ with even integer m, where the round-trip gain g_c from Eq. (14) is real, positive and less than unity, the expressions yield the *minima* of the shift,

$$\frac{\Delta x}{2l}\cong 1-\eta_c\frac{(\eta_c+1)^2+(\eta_c-1)^2\,\exp[-4\kappa_c\omega_c l/c]}{(\eta_c+1)^2-(\eta_c-1)^2\,\exp[-4\kappa_c\omega_c l/c]}$$
$$=1-\eta_c-\frac{2\eta_c g_c}{1-g_c}, \tag{18}$$

and the *maxima* of the mean-square length,

$$\frac{L_T^2}{L^2}\cong 1+\frac{l^2}{L^2}\frac{32\eta_c^2(\eta_c^2-1)^2\exp[-4\kappa_c\omega_c l/c]}{\{(\eta_c+1)^2-(\eta_c-1)^2\exp[-4\kappa_c\omega_c l/c]\}^2}$$
$$=1+\frac{l^2}{L^2}\frac{32\eta_c^2 g_c}{(1-g_c)^2}. \tag{19}$$

These expressions reproduce remarkably well the results shown in Fig. 3, which are obtained from the exact expressions for Δx and L_T^2 derived from Eq. (12). The final term on the right of Eq. (18) takes increasing negative values, larger for amplifiers than for absorbers, as $g_c\to 1$. This gives rise to longer delays ($\eta_c>1$) or shorter advances ($0<\eta_c<1$) for amplified frequencies than for attenuated frequencies. Lengthening of the wave packet with respect to finite or vanishing attenuation can also be seen from Eq. (19) as a result of the higher values of the round-trip gain in amplifying media. Furthermore, it is clear, by comparing Eqs. (18) and (19) for different values of η_c (with fixed κ_c) given by Eq. (15), that an increased delay ($\eta_c>1$) or a reduced advance ($0<\eta_c<1$) always correspond to a lengthening of the pulse.

An analogous discussion can be carried out for the *maxima* of Δx and the *minima* of L_T^2 by considering system parameters for which $4\eta_c\omega_c l/c\cong\pi m$ with odd integer m. The approximate expressions (18) and (19) remain valid, where g_c is again real but now takes negative values. The peak of the transmitted pulse is now advanced, and its length is shortened with respect to finite attenuation and, owing to a negative round-trip gain, the changes are relatively smaller than for even integers. The advances in Fig. 3(a) are largest for $\eta_c>1$ and for the higher value of the amplification with $\kappa_c=-0.04$. When $\eta_c>1$, positive shifts Δx occur for the larger odd-integer values of m, and these represent apparent superluminal behavior with the peak of the pulse transmitted through the slab arriving at an earlier time than the peak of an identical pulse propagated through free space. Apparent superluminal transmission also occurs for $0<\eta_c<1$, although this is mainly associated with the enhanced phase velocity, and the effect of amplification is smaller. Figure 3(b) shows the relatively modest reductions in the length of the wave packet associated with the peak advances.

We now discuss in physical terms how amplification affects the pulse parameters in transmission through the slab. The physical basis is the interference of multiply reflected components of the long pulse inside the narrow slab [2–6]. This can be seen seen by rewriting the complex transmission coefficient $T_c\equiv T(\omega_c)$ defined in Eqs. (6) and (7) as a power series in the internal reflection coefficient at the slab surfaces,

$$T_c=\frac{4n_c\exp(-2i\omega_c l/c)}{(n_c+1)^2}\sum_{j=0}^{\infty}\left(\frac{n_c-1}{n_c+1}\right)^{2j}$$
$$\times\exp\{2(2j+1)in_c\omega_c l/c\}, \quad (20)$$

valid for $|g_c|<1$. The transmitted normal-order Poynting vector for an incident Gaussian pulse is obtained by substitution of Eq. (20) into Eq. (10). Then with the same approximations used in deriving Eq. (12) and for small values of $|\kappa_c|$, the Poynting vector can be written as

$$\langle:\hat{S}(x,t):\rangle\cong S_0\mathscr{T}\left|\sum_{j=0}^{\infty}\left(\frac{n_c-1}{n_c+1}\right)^{2j}\exp\left\{\frac{4ijn_c\omega_c l}{c}\right.\right.$$
$$\left.\left.-\frac{\{x-ct-2l[1-(2j+1)\eta_c]\}^2}{L^2}\right\}\right|^2, \quad (21)$$

where the intensity scaling factor is

$$\mathscr{T}=16|n_c|^2\exp(-4\kappa_c\omega_c l/c)/|n_c+1|^4. \quad (22)$$

When $\kappa_c=0$ and the real refractive index is set equal to unity, $j=0$ is the only nonvanishing term in the sum, and Eq. (21) yields the normal-order Poynting vector associated with the incident pulse. Physically, the sum in Eq. (21) represents the superposition of successive Gaussian wave packets generated by the $2j$-fold internal reflections. The wavepackets have unaltered mean-square lengths L^2, but they are centered on different peak positions. The complex weight associated with each wave-packet component depends on the refractive index η_c and on the attenuating or amplifying value of the extinction coefficient κ_c. The argument and modulus of the complex weight yield, respectively, the phase delay and the effective round-trip gain or loss for light that undergoes j round trips from a point in the slab, and back to the same point before leaving the slab.

The transmitted power density in Eq. (21) includes interference terms arising from superposition of the various wave-packet components inside the slab. These have an important influence in determining the resulting form of the transmitted pulse, and the nature of the interference clearly depends on the phase angle $4\omega_c\eta_c l/c$ between successive contributions to the summation. The nature of the interference is simply illustrated by truncation of the summation after its second term. The first and second terms in the summation represent the transmitted components of the incident pulse after no reflection (primary component) and after two internal reflections (doubly-reflected component), respectively. The shifts in the peaks of these Gaussian components have the values expected from the changes in the optical path length caused by the propagation of the peak of the incident pulse with velocity c/η_c through lengths $2l$ and $6l$ of the dielectric material [2,3]. The product between the first and second terms, representing the interference of the primary and doubly reflected components, is another Gaussian centered halfway between the previous two.

The contributions to the truncated summation from Eq. (21) are shown in Fig. 5 for attenuated and amplified frequencies with pulse and material parameters such that $4\omega_c\eta_c l/c=\pi m$ with $m=24$. In this case the primary and doubly reflected pulse contributions have the same phase,

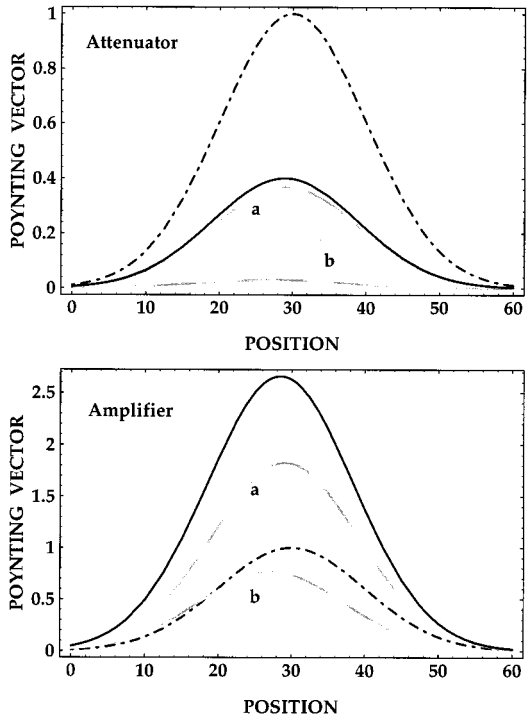

FIG. 5. Power density (21) in units of S_0 as a function of $x/2l$ at time $ct/2l=30$ for a Gaussian pulse of carrier frequency ω_c and initial length L after propagation in free space (dashed black curve) and across a slab of thickness $2l$ (solid black curve), where $\omega_c l/c=10$ and $L=40l$. The upper and lower frames refer to slabs with $\eta_c\cong 1.88$ and $\kappa_c=0.02$ (attenuator) and $\kappa_c=-0.02$ (amplifier). The grey curves show (a) the primary component and (b) the change caused by inclusion of the doubly reflected contribution in Eq. (21). The changes in peak shift $\Delta x/2l$ from the primary value of $1-\eta_c$ are -0.14 (attenuator) and -0.64 (amplifier). The full lengths at half maximum of the transmitted pulse are increased from the incident value by 0.03 (attenuator) and 0.12 (amplifier), in units of $2l$.

and they interfere constructively in the output pulse. The delayed doubly reflected pulse thus enhances the rear part of the envelope of the primary pulse. This superposition produces a pulse reshaping, with the effect of reducing the peak shift Δx of the transmitted pulse below the value $2l(1-\eta_c)$ with a concomitant increase in the length L_T of the transmitted pulse above the incident value L. The second term in the summation in Eq. (21) is very small for attenuated frequencies due to the square of the round-trip loss factor. However, for amplified frequencies, the interference term in Eq. (21) becomes more important, and stronger enhancements of the rear part of the pulse occur: this causes larger reductions of the pulse shift and greater increases in the pulse width than occur for attenuated frequencies.

When the system parameters are chosen so that $4\omega_c\eta_c l/c=\pi m$ with $m=23$, the primary and doubly reflected pulse contributions have opposite phases, and they interfere destructively in the output pulse. The delayed doubly reflected pulse thus weakens the rear part of the envelope of the primary pulse. The superposition thus has the effects of increasing the peak shift Δx of the transmitted pulse above the value $2l(1-\eta_c)$ and reducing the pulse length L_T below the incident length L, as shown in Fig. 6. The effects are again greater for amplified frequencies than for attenu-

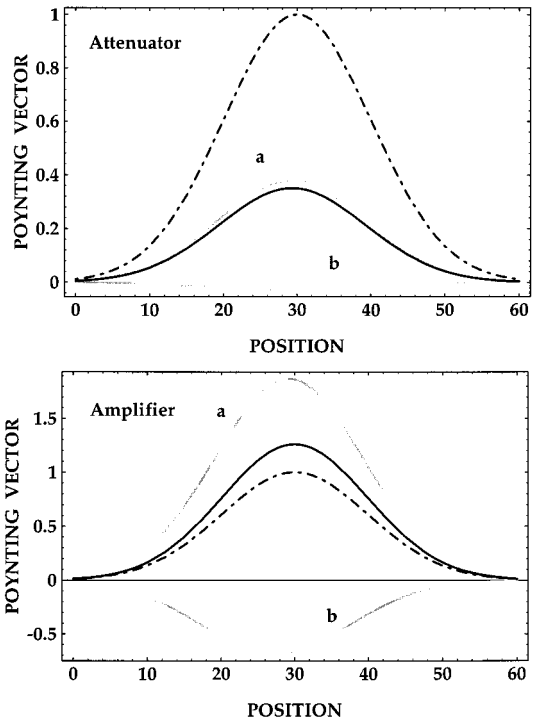

FIG. 6. The same as in Fig. 5, but with $\eta_c \cong 1.81$. The changes in peak shift from the primary value are 0.14 (attenuator) and 0.79 (amplifier). The full lengths at half maximum are reduced from the incident value by 0.02 (attenuator) and 0.20 (amplifier) in units of $2l$.

ated frequencies. The changes in the values of the peak shift and pulse width obtained from Eq. (21) agree approximately with those shown in Fig. 3; closer agreement is achieved by including a larger number of terms in the summation.

It is seen from Figs. 5 and 6 that the spatial distributions of the transmitted pulses always lie within the spatial range of the incident pulse. The apparent peak delay or advance and the broadening or narrowing of the transmitted pulse with respect to the incident pulse are consequences of the reshaping caused by interference of the multiply reflected components that make up the transmitted pulse. In particular, any apparent superluminal transmission is produced by destructive interference in the rear of the pulse and no part of the pulse intensity travels faster than light, as has been pointed out previously in related systems [5–8].

V. CONCLUSIONS

We have derived the effects of propagation through a dielectric slab on a Gaussian optical pulse that is much longer than the slab thickness, when the transmitted pulse retains its Gaussian shape. For transparent dielectric material with negligible dispersion, the propagation causes changes in the peak position and length of the transmitted pulse with respect to those of the incident pulse. These changes result from the interference between multiply reflected contributions and the primary component that travels through the slab without any reflections at its surfaces. When the reflected contributions have the same phase as the primary component, their effect is to enhance the rear of the primary pulse, with a lengthening and peak delay of the composite transmitted pulse. When the first, or doubly reflected, contribution has opposite phase to the primary component, its effect is to dimish the rear of the primary pulse; this effect persists when the higher-order multiply reflected contributions are included, leading to a shortening and peak advance of the transmitted pulse.

The strengths of the multiply reflected contributions are reduced when the dielectric material attenuates light at the carrier frequency of the pulse. We have previously evaluated the associated reductions in the magnitudes of the peak shift and length changes of the transmitted pulse [6]. By contrast, it would be expected that amplification of light at the carrier frequency should increase the strengths of the multiply reflected contributions and enhance the changes in pulse peak position and length relative to their values for a transparent dielectric. We have shown in the present paper that this is indeed the case, and have presented analytic and numerical results for the magnitudes of the changes in the pulse position and length. The analytic results are valid when the magnitude of the negative extinction coefficient is much smaller than unity. They confirm the interpretation of the pulse reshaping as a consequence of the interference of the primary pulse with multiply reflected contributions, as is clearly demonstrated by the data shown in Figs. 5 and 6. The numerical results apply more generally, but with the restriction that the magnitude of the extinction coefficient should not be large enough to cause self-sustaining laser oscillation of the slab at any of the amplified frequencies.

The variations of the peak shift and mean-square length of the transmitted pulse shown in Fig. 3 still refer to modest magnitudes of the extinction coefficient, but they include ranges of round-trip gains g_c that approach lasing thresholds. It is seen that the presence of amplification produces striking increases in the amplitudes of oscillation relative to the transparent dielectric. The minima in Δx and the maxima in L_T correspond to multiply reflected components that are all in phase, and the system thus tends to the achievement of laser action for sufficiently high gain. The magnitudes of the peak shift and the pulse width both increase without limit as the round-trip gain tends to unity, and the pulse is replaced by continuous emission at the laser threshold. The maxima in Δx and the minima in L_T correspond to multiply reflected components that alternate in phase; laser action cannot be achieved in these conditions, but the pulse transmission tends to superluminal behaviour for gains sufficiently high to remove significant amounts of the rear of the pulse by destructive interference. Our interpretation of these phenomena thus agrees with the proposal that interference between successive components of the transmitted pulse is the common source of apparent superluminal behavior in propagation through dielectric structures, however complicated [5].

Observations of a pulse transmitted through an amplifying medium must be made against the inevitable noise background represented by Eq. (8) and discussed more fully in Refs. [6] and [14]. The use of quantum theory is necessary for proper inclusion of the noise, whose effects can be mitigated in practice by appropriate spectral and temporal filtering. However, for the reshaping effects on a transmitted Gaussian pulse, a classical calculation involves essentially the same integration as carried out in Eq. (10) for the Gaussian photon-number wave packet treated here, and the same results would be obtained. Measurements of pulse transmis-

sion use the interference between photons propagated through the slab and through free space [1]; attenuation in the material of the slab modifies this two-photon interference [21] and analogous modifications, not considered here, should occur for amplifying media.

The pulse reshapings derived here are consequences of the combined effects of multiple reflections of the incident pulse and of its amplification inside the slab. Dispersion in the dielectric properties has been ignored, and the group velocity has been set equal to the phase velocity. It is well known that the variations in the group velocity have important effects on pulse transmission through attenuating dielectrics, including apparent superluminal behavior, when the pulse frequency lies close to a dielectric resonance [22,23]. Similar effects are expected to occur for pulse frequencies close to resonances in amplifying dielectrics [9–14]. The calculations of the present paper assume a pulse carrier frequency well removed from dielectric resonances, where the dispersion is negligible. They show that a wealth of phenomena occur even for pulse propagation through nonresonant amplifying media.

ACKNOWLEDGMENTS

We thank the European Community Human Capital and Mobility Programme and the Ministerio de Educacion y Cultura of Spain for financial support.

[1] A. M. Steinberg, P. G. Kwiat, and R. Y. Chiao, Phys. Rev. Lett. **71**, 708 (1993).
[2] P. Halevi and R. Fuchs, Phys. Rev. Lett. **55**, 338 (1985).
[3] P. Halevi, Opt. Lett. **11**, 759 (1986).
[4] P. Halevi and L. D. Valenzuela, J. Opt. Soc. Am. B **8**, 1512 (1991).
[5] Y. Japha and G. Kurizki, Phys. Rev. A **53**, 586 (1996).
[6] M. Artoni and R. Loudon, Phys. Rev. A **55**, 1347 (1997).
[7] T. Gruner and D.-G. Welsch, Acta Phys. Slov. **46**, 387 (1996).
[8] T. Gruner and D.-G. Welsch, Opt. Commun. **134**, 447 (1997).
[9] R. Y. Chiao, Phys. Rev. A **48**, R34 (1993).
[10] E. L. Bolda, R. Y. Chiao, and J. C. Garrison, Phys. Rev. A **48**, 3890 (1993).
[11] A. M. Steinberg and R. Y. Chiao, Phys. Rev. A **49**, 2071 (1994).
[12] E. L. Bolda, J. C. Garrison, and R. Y. Chiao, Phys. Rev. A **49**, 2938 (1994).
[13] R. Y. Chiao, A. E. Kozhekin, and G. Kurizki, Phys. Rev. Lett. **77**, 1254 (1996).
[14] E. L. Bolda, Phys. Rev. A **54**, 3514 (1996).
[15] D. L. Fisher and T. Tajima, Phys. Rev. Lett. **71**, 4338 (1993).
[16] L. Casperson and A. Yariv, Phys. Rev. Lett. **26**, 293 (1971).
[17] R. Matloob, R. Loudon, S. M. Barnett, and J. Jeffers, Phys. Rev. A **52**, 4823 (1995).
[18] J. Jeffers, S. M. Barnett, R. Loudon, R. Matloob, and M. Artoni, Opt. Commun. **131**, 66 (1996).
[19] R. Matloob, R. Loudon, M. Artoni, S. M. Barnett, and J. Jeffers, Phys. Rev. A **55**, 1623 (1997).
[20] C. K. Hong, Z. Y. Ou, and L. Mandel, Phys. Rev. Lett. **59**, 2044 (1987).
[21] J. Jeffers and S. M. Barnett, Phys. Rev. A **47**, 3291 (1993).
[22] C. G. B. Garrett and D. E. McCumber, Phys. Rev. A **1**, 305 (1970).
[23] S. Chu and S. Wong, Phys. Rev. Lett. **48**, 738 (1982).